Characterization of a novel interaction partner of lysosomal GTPase Arl8b

Sahil Kamboj

A dissertation submitted for the partial fulfillment of BS-MS dual degree in Science

Indian Institute of Science Education and Research
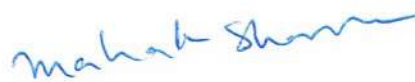
Mohali

May 2020

Certificate of Examination

This is to certify that the dissertation titled **"Characterization of a novel interaction partner of lysosomal GTPase Arl8b"** submitted by Mr. Sahil Kamboj (Reg. No. MS15006) for the partial fulfillment of BS-MS dual degree program of the Institute, has been examined by the thesis committee duly appointed by the Institute. The committee finds the work done by the candidate satisfactory and recommends that the report be accepted.

Dr. Indranil Banerjee   **Dr. Sharvan Sehrawat**   **Dr. Mahak Sharma**
                                                                          (Supervisor)

Dated: May 4th, 2020

Declaration

The work presented in this dissertation has been carried out by me under the guidance of Dr. Mahak Sharma at the Indian Institute of Science Education and Research, Mohali.

This work has not been submitted in part or in full for a degree, a diploma, or a fellowship to any other university or institute. Whenever contributions of others are involved, every effort is made to indicate this clearly, with due acknowledgement of collaborative research and discussions. This thesis is a bonafide record of original work done by me and all sources listed within have been detailed in the bibliography.

Sahil Kamboj

(Candidate)

May 04, 2020

In my capacity as the supervisor of the candidate's project work, I certify that the above statements by the candidate are true to the best of my knowledge.

Dr. Mahak Sharma

(Thesis supervisor)

Acknowledgment

I express my sincerest gratitude towards my project guide Dr. Mahak Sharma, who accepted me as a Masters' thesis student and allowed me to have an experience of a lifetime in her lab. I wholeheartedly thank her for all the intellect and wisdom she shared throughout my thesis project. Through her valuable feedback and vital life lessons, she has inspired me to be a thorough academician, professional, and a humble person. I could not have imagined a better mentor for my Masters' thesis. My sincere thanks also go to Dr. Lolitika Mandal, Dr. Sudip Mandal, and Dr. Maithreyi Narasimha for offering me summer internship opportunities and helping me to develop my scientific temper.

This project would not have been possible without the constant support and encouragement of Dr. Mahak's lab members. I am incredibly thankful to Ms. Shalini Rawat for her consistent support and guidance for mastering the techniques in the lab. Her infectious enthusiasm inspired me to work harder whenever I was stuck. Her fun-filled teasing, along with the endless discussions of daily soaps, made working alongside her joyous and exciting. I am grateful to other fellow lab members – Ms. Sankalita and Ms. Neha, for their assistance. I am thankful to them for helping me to cross the wall. I thank Mrs. Kanupriya Sethi for being an excellent lab assistant and sharing her valuable life experiences from time to time. I thank my fellow Masters' students in the lab - Amit and Gitanjali for helping me with my work and maintaining a positive work environment. I would also like to thank Shabduli, Shrestha, Sanjeev, and Ayush Jain for their motivation, support, and help in the work.I thank Mr. Baidnath Mandal (Vidya Bhaiya) for his efforts and hard work as a lab technician.Many thanks to my friend Ananya for her never-ending belief in me and my hard work. I thank her for sharing all the witty suggestions and tea-break discussions for stress detours. I am immensely grateful to Surendra, Bhavya, Ayush, Saurabh, and Rajesh for giving me moments to cherish and building unforgettable memories.

I also thank my parents, Mrs. Santosh Kamboj and Mr. Jai Chand Kamboj and my sister, Ms. Aashima Kamboj, for believing in me and providing me with all that was needed throughout my BS-MS journey. I thank my thesis committee members Dr. Indranil Banerjee and Dr. Sharvan Sehrawat, for reviewing this report. Last but not least, I duly acknowledge the efforts put in by the faculty members and the non-teaching staff of IISER Mohali, who have guided and helped me throughout the last five years.

List of Figures

Abbreviations

Arl8b	ADP-ribosylation factor-like protein 8B
BORC	BLOC-1 related complex
HOPS	Homotypic fusion and sorting protein
PLEKHM1	Pleckstrin homology domain-containing family member 1
SKIP	SifA and kinesin-interacting protein
RILP	Rab-interacting lysosomal protein
FYCO	FYVE and Coiled-coil domain containing protein 1
SNARE	Soluble N-ethylmaleimide-sensitive factor-attachment protein receptor
VAMP7	Vesicle-associated membrane protein 7
TBC1D9B	Tre2/Bub2/Cdc16 – 1 domain family member 9B
LB	Luria Broth
IPTG	Isopropyl-β-D-1-thiogalactopyranoside
PFA	Paraformaldehyde
PBS	Phosphate buffered saline
EDTA	Ethylenediaminetetraacetic acid
PHEM	PIPES, HEPES, EGTA, $MgCl_2$
GST	Glutathione-S-transferase
SDS-Page	Sodium dodecyl sulphate – Polyacrylamide Gel electrophoresis
DMEM	Dulbecco's modified Eagle medium
FBS	Fetal Bovine Serum
LAMP1	Lysosome associated membrane protein 1
EEA1	Early endosome antigen 1
M6PR	Mannose-6-phosphate receptor

Contents

Abstract

Chapter 1

Chapter 2

Chapter 3

Chapter 4

Abstract

Vesicular trafficking in eukaryotic cells is tightly regulated by various families of small GTP binding proteins, including Rabs, Arfs, and Arf-like (Arl) proteins. Small GTP binding protein Arl8b is known to regulate lysosome motility and function in mammalian cells. Arl8b is recruited onto the lysosomes by BORC, and by interacting with various effectors, it governs essential cellular functions. Interaction of Arl8b with SKIP helps in the motility of lysosomes from minus end to the plus end of the microtubules. Arl8b also helps in late endosome-lysosome as well as autophagosome-lysosome fusion by interacting with proteins like HOPS and PLEKHM1. Since we now know that Arl8b has many effectors, it is crucial to establish novel interaction partners and effectors of Arl8b to better understand lysosome biology. The objective of the study was to characterize a possible novel interaction partner of small GTP binding protein Arl8b.

In this study, we determined a novel interaction partner of lysosomal GTPase Arl8b, which is a member of Tre2/Bub2/Cdc16 family of proteins. Our preliminary observations indicate that upon RNAi depletion of this novel interaction partner, LAMP1, Rab14,and Rab7 compartments generally appear enlarged. Immunostaining for M6PR shows more endosomal staining for this cargo; moreover EEA1 also appears to be on enlarged endosomes. Our observations suggest that this protein interacts with Arl8b and may regulate the endo-lysosomal pathway. The detailed cellular roles and mechanism of action of this TBC protein need to be investigated in future studies.

Chapter 1

Introduction

1.1 Transport Pathways in a Eukaryotic Cell

Eukaryotic cells are highly compartmentalized with various membrane-bound compartments present in them. Various events occur in the cell including the synthesis of macromolecules, transportation of cellular cargo either directly or packed in vesicles, and degradation and recycling of degraded material for new synthesis. Evolution has enabled the eukaryotic cells to compartmentalize and enable efficient separation of these cellular functions. However, communication of the cell with its environment and within different compartments is essential for the development of the cell. Major part of the communication between the intracellular compartments is achieved by vesicular transport which is tightly regulated and directional. This transport takes place by budding off of a cargo-loaded vesicle from the donor compartment and it's fusion with the acceptor compartment. Different trafficking pathways and transport routes are connected and governed by vesicular transport.

One of the pathways which is crucial for cell communication and signaling is the Endocytic pathway. It involves the internalization of cargo; it's delivery to the early endosomes and further recycling or degradation of endocytosed contents. Once internalization

Figure 1.1 Endolysosomal network. The endocytosed vesicles are delivered to the early endosomes where they are sorted and delivered to different pathways. Adapted from Peter Cullen et al Nature Reviews Molecualr Cell Biology 2018.

happens, the internalized molecules are delivered to the early endosomes which act as a single point sorting station for different destinations (Gruenberg Jean, et al 2001).

Early endosomes are highly dynamic and pleiomorphic in nature as they can have distinct cisternal, tubular and multivesicular regions. Endocytosed materials from the early endosomes are directed either to the recycling pathway or the degradative pathway. Thus, some of the receptors and proteins are recycled back to the plasma membrane via the recycling endosomes whereas the contents destined for degradation are delivered to late
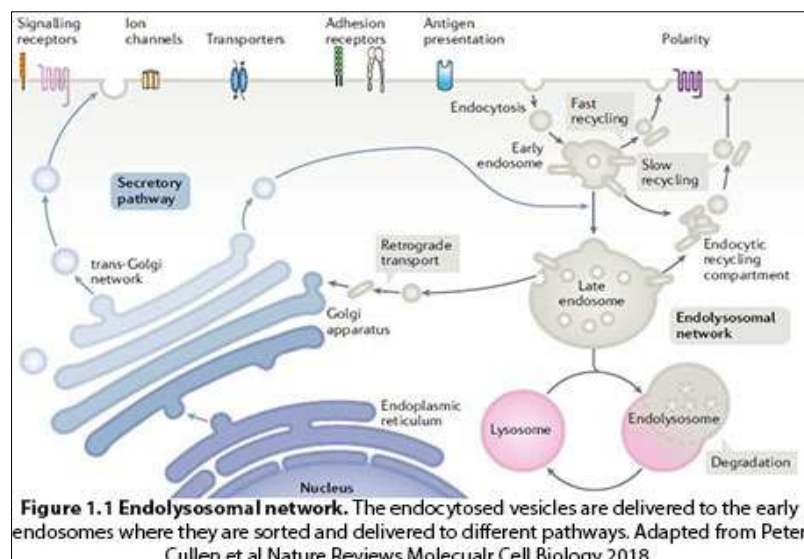
endosomes and lysosomes. Each step of trafficking is regulated by families of endocytic regulatory proteins; prominent amongst these are the small GTP-binding (G) proteins and their effectors.

1.2 Small GTP binding proteins in Endocytic Pathways

Small GTP binding proteins act as key factors in the regulation of cellular trafficking and dynamics. They alternate between two conformations in the cell – the membrane-localized GTP bound form and the cytosolic GDP bound form. This cyclical switching is governed by the activity of Guanine Nucleotide Exchange Factors (GEFs) and GTPase Activating Proteins (GAPs).In their
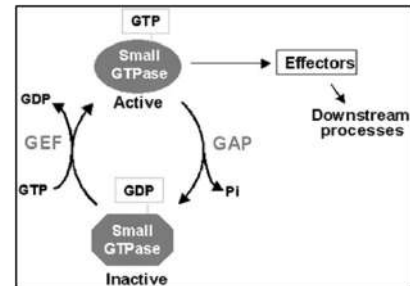
Figure 1.2 (a) Small GTPase Cycle

GTP bound state, small GTP binding proteins recruit various effector proteins and mediate downstream processes. The active form is then converted into inactive GDP bound form by the activity of GAPs. The inactive form is thereafter maintained in the cytosol by Guanine Nucleotide dissociation inhibitors (GDI) which specifically bind to the GDP-bound form and inhibit the release of GDP. Further when required, GEFs mediate the exchange of GDP to GTP and help in transitioning of small G-proteins into their active membrane-bound state.

Of all the small G-proteins, Ras superfamily is most prominent. Members of Rab, Arf and

Figure 1.2(b) Intracellular localization of Rab proteins. Rabs associate with distinct sub-cellular compartments and help in intracellular trafficking. Adapted from Zerial et al 2001

Arf-like (Arl) GTP binding proteins of the Ras superfamily act as key molecular players in intracellular trafficking. Besides these, Rho, Ran, Rap, Rad, Rheb and Miro subfamilies are also being characterized and studied extensively (Song, Siyang, et al). Among these subfamilies, Rab family of proteins is known to regulate various steps of trafficking in the endocytic pathway. For example (Figure 1.2b) Rab5 mediates the traffic from the plasma membrane to the early endosomes, Rab7 is well defined to direct the traffic towards the late endosomes and Rab4, Rab11 and Rab35 are known to mediate the recycling pathway.

1.3 Small G-proteinsat the Lysosome

Arl8b is a member of Arl family of small G proteins that is present on lysosomes and regulates cellular lysosome distribution and functioning. It is highly conserved across different taxonomic groups including protozoans, metazoans as well as plants. Arl8b is different from other Arf proteins in the sense that a conserved glycine residue at the second position is replaced by leucine (Donaldson & Jackson et al., 2011). Though much has been studied about Arl8b, it's GEF and GAP remain undiscovered.

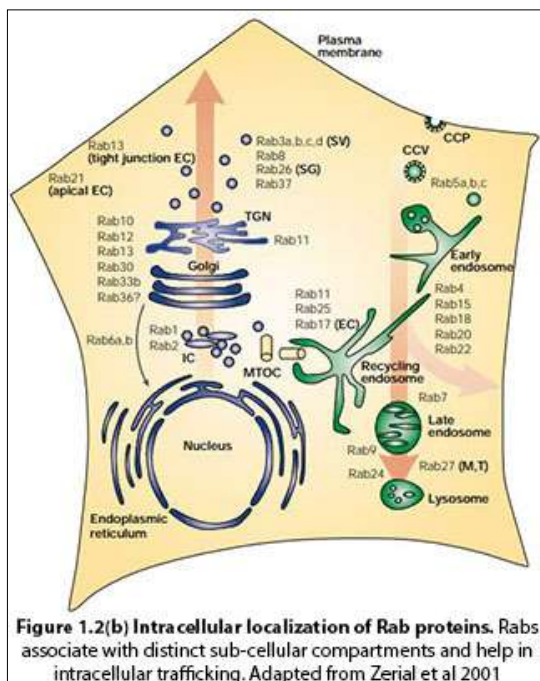Previous studies show that the anterograde transport of lysosomes is mediated by BORC (BLOC-1 related complex), Arl8b-SKIP and kinesin-1 complex (Figure 1.3). BORC is associated on the cytosolic face of the lysosomes and is responsible for the recruitment of small G-protein Arl8b on the surface of lysosomes (Pu et al., 2015). Thereafter, Arl8b interacts with SKIP/PLEKHM2, which in turn binds to motor protein kinesin-1 and this association helps in the motility of lysosomes towards the cell periphery (Rosa-Ferreira and Munro, 2011; Bagshaw et al, 2006). Besides Arl8b and its effectors, Rab7 and its effector on ER membrane namely, Protrudin transfers lysosomes to another Rab7 effector, FYCO1, which associates with kinesin-1 and transports lysosomes towards cell periphery (Raiborg et al., 2016; Matsuzaki et al., 2011). On the other hand, Rab7 has also been implicated in the retrograde transport of lysosomes towards the nucleus. Rab7 recruits RILP on the late endosomes/lysosomes, which in turn binds to dynein-dynactin machinery to transport lysosomes towards the perinuclear region.
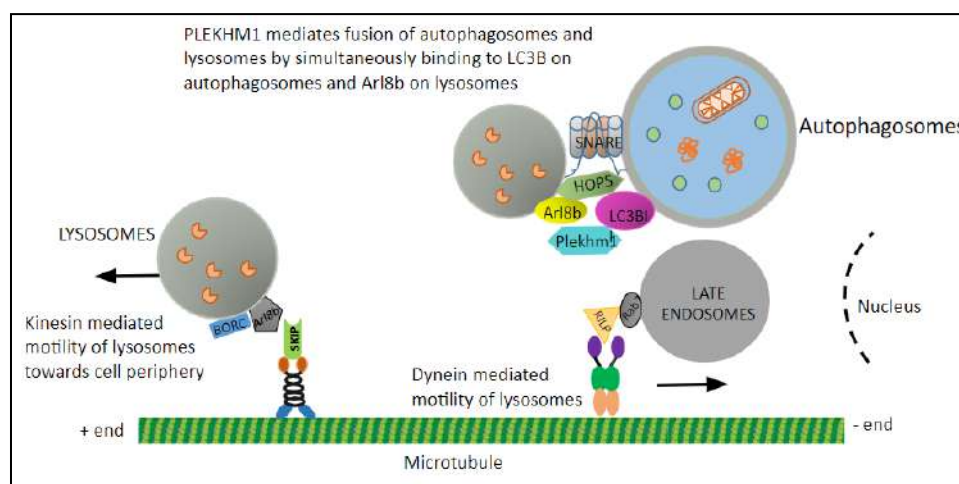
Figure 1.3 Lysosome motility and functioning. Rab7 and Arl8b play crucial roles in regulating lysosome distribution and lysosomal degradation pathway. Image Courtsey – Ms. Shalini Rawat

Both Rab7 and Arl8b are also implicated in the interactions of late endosomes and lysosomes. The delivery of endocytosed cargo to lysosomes by the late endosomes can occur either by kiss-and-run events or by fusion of the two compartments. Fusion of late endosome and lysosome requires a tethering complex- HOPS, and trans-SNARE

complex. Arl8b and Rab7-RILP recruit HOPS complex to lysosomes, promoting tethering of late endosome-lysosome membranes (Khatter et al., 2015; van der kant et al., 2013).The fusion event results in the formation of a hybrid organelle in which endocytosed macromolecules are degraded. Lysosomes can also be re-formed from these hybrid organelles (Bright NA et al., 1997).On the other hand, the fusion of autophagosome and lysosome (Figure 1.3) requires interactions of HOPS complex, PLEKHM1, SNAREs (STX17, VAMP8 & SNAP29), LC3B and small GTP binding protein Arl8b (Lőrincz, P., & Juhász, G. et al 2019). Thus, Arl8b and Rab7 act as crucial regulators of lysosome function as well as their distribution.

Our research group is interested in exploring the role of small GTP binding protein Arl8b in lysosomal functioning and determining its novel effectors and interaction partners. To this end, we identified novel interaction partners of Arl8b by using GST-Arl8b as bait to pull down interaction partner from mammalian. Mass spectrometry of the eluate revealed TBC1D9B as one of the positive hits. The main aim of this study was to pursue TBC1D9B protein as a possible interaction partner of Arl8b and characterize its roles in the cell. Below I describe what are TBC domain-containing proteins and role of the TBC domain followed by a summary of literature on TBC1D9B.

1.4 TBC family of proteins

The conversion of Rab-GTP to GDP form is regulated by GAPs (Section 1.2). Many GAPs for Rab proteins contain a characteristic Tre2/Bub2/Cdc16 (TBC) domain which is usually (not always) the Rab-binding domain (Richardson and Zon, 1995). TBC domain is around 200 amino acids long and it conserved in all eukaryotes. TBC domain-containing proteins (TBC proteins) were initially identified and described independently of Rab GTPases. Establishing TBC proteins as putative Rab GAPs opened a bundle of opportunities to determine the Rab substrates of different TBC proteins and to get better mechanistic insights at the functioning of these proteins.

Initially, the identification of Rabs of TBC proteins primarily depended on their physical interactions. However, subsequent studies have established that the GAP activity of TBC proteins does not always require a close physical interaction. Complications in identifying Rab substrates for TBC proteins arise from the fact that not all TBC proteins have their primary role as Rab-GAPs. The Rab-GAP function of TBC proteins depends on two conserved motifs in the TBC domain - an arginine or R finger within an IxxDxx**R** motif, and a glutamine or Q finger within an **Y**x**Q** motif. The Y residue of Q finger interacts

with the glutamate of the Rab GTPase while the R and Q residues coordinate with Rab-bound GTP and promote its hydrolysis. (Pan *et al.*, 2006; Gavriljuk *et al.*, 2012). Catalytic arginine mutants and RYQ triple mutants of TBC proteins act as powerful tools for the screening of Rabs involved in intracellular trafficking. However, approx. a quarter of TBC proteins lack this conserved arginine residue and are unlikely to act as Rab-GAPs. Most members of the TBC protein family still remain poorly studied.

Despite these challenges, many TBC proteins with GAP activity have been implicated as regulators of intracellular membrane trafficking, including autophagy. TBC1D5, TBC1D10A, TBC1D14, and TBC1D25, are known to regulate starvation-induced autophagy (Minowa-Nozawa & Nagakawa et al 2017; Longatti, A. et al. 2012; Popovic, D. et al 2012; Itoh et al 2011), whereas TBC1D15 and TBC1D17 (Yamano & Kogel et al 2014) are required for mitophagy, and TBC1D10A is involved in xenophagy and mitophagy (Minowa-Nozawa & Nagakawa et al 2017).

1.5 TBC1D9A/B – TBC domain-containing protein

TBC1 domain family member 9 has two paralogues – TBC1D9A and TBC1D9B. The domain architecture of both these proteins is similar. TBC1D9A is 1266 amino acids long whereas TBC1D9B contains 1250 amino acids (differing in 16 amino acids in the N-terminus region). TBC1D9A/B both proteins contain two GRAM domains, one TBC domain (including the R and Q fingers) and a C-terminal E-F Hand motif each (Doerks et al., 2000; Frasa et al., 2012) (Figure 1.6 a). Explicit functions of these domains have not been characterized yet. In general, the GRAM domains are thought to be protein/lipid binding signaling domains. TBC domain in some TBC proteins has been shown to bind to Rab proteins and govern the Rab-GAP activity. The E-F hand motif is known to fold into the helix-loop-helix structure and act as a calcium ion binding motif.

Figure 1.5 (a) Domain architecture of TBC1D9A and TBC1D9B. Domain information was extracted from NCBI, images were made using the DOG software.
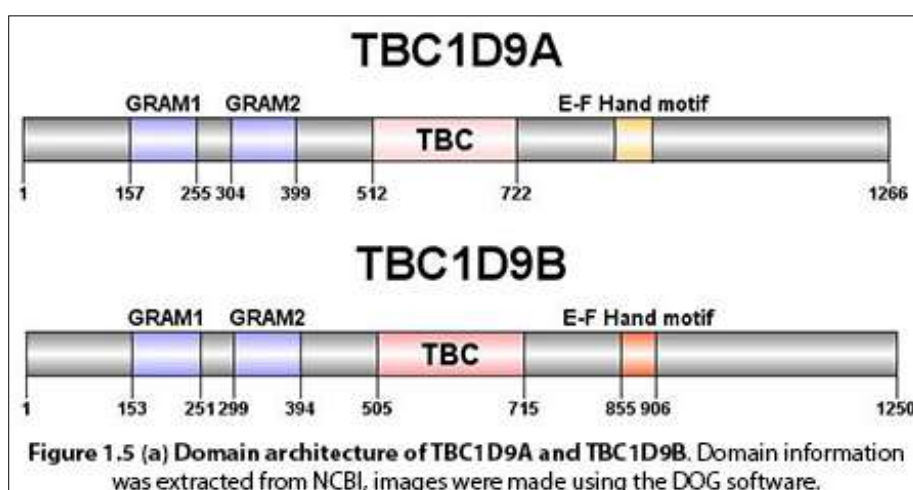
TBC1D9 proteins have homologs in other well-known model organisms as well. Besides this, TBC1D9B has two isoforms – longer isoform (a) and shorter isoform (b). Amino acid sequence similarity alignment done between the orthologs of TBC1D9 proteins in various organisms showed generally >50% similarity between the sequences. This observation indicates that TBC1D9A and B have remained conserved across evolutionarily time scales and thus might play an important role in the cell (Figure 1.6 b).

	hTBC1D9A	hTBC1D9B(a)	hTBC1D9B(b)	Danio rerio TBC1D9	C. elegans tbc-9	Drosophila melanogaster CG7324
hTBC1D9A	100	74.6	75.2	87.7	49.9	50.3
hTBC1D9B(a)	74.6	100	98.6	74.9	50.5	46.7
hTBC1D9B(b)	75.2	98.6	100	74.8	50.5	47.2
Danio rerio TBC1D9	87.7	74.9	74.8	100	50.1	50.1
C. elegans tbc-9	49.9	50.5	50.5	50.1	100	48.9
Drosophila melanogaster CG7324	50.3	46.7	47.2	50.1	48.9	100

Figure 1.5 (b) Amino acid sequence similarity alignment of TBC1D9 homologs. Sequences of homologs were extracted using BLAST and NCBI. Alignment was done using the EMBOSS tool 'Needle'.

Published literature on TBC1D9B protein is very limited. TBC1D9B has been shown to act as a GAP for Rab11A in a canine cell line (Fukuda et al 2014). Another report on TBC1D9B has shown that it interacts with LC3B and positively regulates autophagic flux (Liao et al 2018). One recent report also suggests that the paralogue TBC1D9 regulates TBK1 (TANK-binding kinase 1) activation in response to microbial infection by binding Ca^{2+} through the E-F hand motif in selective autophagy (Nozawa, Sano, Minowa-Nozawa *et al* 2020). TBC1D9 has also been suggested to be involved in male breast carcinomas (Andres, S.A. et al 2012) Furthermore, sub-cellular localization and other roles and mechanism of action of TBC1DB need to be investigated. Another recent article reported that GFP-TBC1D9A showed localization to Rab7 endosomes in HEK293-AT1 cells and GFP-TBC1D9B caused the Rab7 endosomes to localize to the cell periphery. This article also showed that the independent knockdowns of TBC1D9A and TBC1D9B caused defects in the fusion of autophagosomes and lysosomes (Baba, T. et al 2019). All these published reports suggest a role of TBC1D proteins in the endo-lysosomal pathway. We did a mass spectrometric analysis to discover novel interaction partners of Arl8b and got TBC1D9B as a candidate. We further confirmed the interaction of Arl8b with TBC1D9B by GST pull down assays. To further define the roles of TBC1D9B, we did RNAi depletion of TBC1D9B and analyzed different intracellular compartments using

well-characterized markers of these compartments, such as LAMP1 (lysosomes), Rab7 (late endosomes/lysosomes), Rab14 (early endosomes/Golgi), EEA1 (early endosomes) and CI-M6PR (endosomes, golgi). Our observations indicate that various compartments along the endo-lysosomal pathway are affected upon TBC1D9B knockdown. Thus, we propose that TBC1D9B plays a role in the endo-lysosomal network. Determination of detailed mechanism of action and other roles of TBC1D9B shall be pursued in future studies.

Chapter 2

Methods and Materials

2.1 Materials

2.1.1 Plasmids and Constructs

Myc tagged TBC1D9B construct was subcloned from TBC1D9B-pGADT7 and a myc tag was added at the N terminus of full-length TBC1D9B. pcDNA3.1(-) vector used to clone TBC1D9B with myc tag.

2.1.2 Media

Ultrapure type 1 water was used for preparing all the buffers and media. Sterilization was done by autoclaving before use.

<u>LB Media:</u> Luria Broth Powder was used for making LB Media. 2.5g of the powder was added in 100mL of type 1 water and autoclaved before use.

<u>Superbroth Media:</u>1.2g of Tryptone, 2.4g of Yeast Extract and 400μL of 100% glycerol was added to make up the volume till 90mL with Type1 water. The media was autoclaved and 10mL of previously prepared salt solution was added to the media before use.

<u>SOB Broth</u>: 50mg of NaCl, 2g of tryptone, 0.5g of yeast extract, 18.6mg of KCl and 203.3mg of $MgCl_2$were dissolved in 100mL of type 1 water and the media was autoclaved before use.

2.1.3 Buffers and stock solutions

All the buffers and stock solutions were prepared as per the following compositions:-

<u>Transformation Buffer #1</u> - For 100mL of transformation buffer #1, 10mM of MOPS (pH 6.5), 100mM of KCl, 45mM of $MnCl_2$, 10mM of $CaCl_2$ and 10mM of potassium acetate (pH 7.5) were added as per the calculations and the final volume was made upto 100mL.

<u>Transformation Buffer #2</u> - For 100mL of transformation buffer #2, 10mM of MOPS (pH 6.5), 100mM of KCl, 45mM of $MnCl_2$, 10mM of $CaCl_2$ and 10mM of potassium acetate (pH 7.5) were added as per the calculations from the stock solutions and

dissolved in around 60mL of type 1 water. Then, 12.5mL of glycerol was added and the final volume was made upto 100mL.

Transformation Buffer #3 - A buffer containing a final concentration of 100mM of $CaCl_2$ and 50mM of $MgCl_2$ was prepared in type 1 water as per need.

50X TAE:242g of Tris-base was dissolved in 700mL of autoclaved type 1 water and then 57.1mL of 100% glacial acetic acid and 100mL of 0.5M EDTA (pH 8.0) was added to it. The final volume was adjusted to 1 liter.

Prep Buffer for protein purification:Buffer with working concentrations of 20mM Tris-Cl (pH 8.0), 150mM NaCl, 0.5% Triton-X 100 and 5% glycerol was made using autoclaved type 1 water as per the calculations. Two tablets of Roche Protease Inhibitor were added for 100mL buffer and 1mM working concentration of PMSF was used.

TAP Lysis Buffer: 2mL of 1M Tris-Cl (pH 8.0), 15mL of 1M NaCl, 200µL of 0.5M EDTA, 50µL of 1M DTT, 5mL of 10% Triton-X and 5mL of 100% glycerol was added to autoclaved type 1 water to make final volume of 100mL. Two tablets of Roche PI cocktail were added along with 1mL of 100mM PMSF.

10X SDS Gel Running Buffer: 144g glycine, 30.2g Tris base and 10g powdered SDS was dissolved in 600mL of type 1 water. The solution was nixed properly until it becomes clear and then the volume was made up to 1 literusing type 1 water.

1X Transfer Buffer: 6g of Tris base, 28.5g glycine and 400mL of methanol were dissolved in type 1 water and used to make a total of 2 litres of ready to use 1X transfer buffer. The buffer was stored at 4°C until further use.

Resolving Gel Buffer:36.342g of Tris base was added to 100mL of autoclaved type 1 water. After Tris gets dissolved in the water completely, set the pH of the buffer to 8.8 using HCl. Make up the final volume to 200mL using autoclaved type 1 water.

Stacking Gel Buffer:12.114g of Tris base was added to 100mL of autoclaved type 1 water. After Tris gets dissolved in the water completely, set the pH of the buffer to 6.8 using HCl. Make up the final volume to 200mL using autoclaved type 1 water and filter the buffer before use.

10X phosphate-buffered saline (PBS):2 g KCl, 80 g NaCl, 2.4 g KH_2PO_4, 14.4 g Na_2HPO_4 were dissolved in 800 mL of Type 1 water. The volume made up to a liter and the buffer was filtered and autoclaved. 1X PBS was prepared from 10X PBS stock and its pH was adjusted to 7.4 before use.

0.05% and 0.3% PBST:2.5mL of 20% Tween-20 was added to 1X PBS and the volume was made upto 1 liter using 1X PBS to make 00.5% PBST. Similarly, 15mL of 20% Tween-20 was added to 1X PBS and volume was made upto 1 liter using 1X PBS.

16% paraformaldehyde (PFA):16 g paraformaldehyde was dissolved in 70 ml of PBS (1X) at 40-60°C by adding 1 M NaOH till the solution turned transparent. The pH of the solution was adjusted to 7.4 and the volume was made up to 100 mL. Aliquots of 2mL were made and stored at -20°C. 4% working PFA was made (in PHEM Buffer) from 16% PFA as and when required.

2.1.3 Antibodies

Anti-myc mouse monoclonal antibody (sc-40 9E10) was purchased from Santa Cruz Biotechnology, USA and used for western blotting experiments with 1:1000 dilution. Anti-LAMP1 rabbit (ab24170), anti-Rab14 rabbit, anti-(Transferrin receptor) rabbit and anti-M6PR rabbit antibodies were purchased from abcam (UK). Anti-GM130 mouse (610823) and anti-EEA1 mouse (610456) antibodies were purchased from BD Biosciences. Anti-Rab7 mouse antibody (sc-376362) was procured from SantaCruz Biotechnology and anti-LC3 rabbit antibody (PM036) was purchased from MBL Ltd. (Japan). All the Alexa fluorophore-conjugated secondary antibodies were purchased from Life Technologies. HRP-conjugated goat anti-mouse and goat anti-rabbit were purchased from Jacksons Immuno Research Laboratories.

2.1.4 siRNA oligos and RT PCR reagents

For gene silencing, siRNA oligos were purchased from Dharmacon and prepared according to the manufacturer's manual. Sequences of the oligos are as follows:-
Control siRNA seq

Sense Seq - GGGCAAAGAGUGAGAGAUAUU

Anti-Sense Seq - UAUCUCUCACUCUUUGCCCUU

hTBC1D9B 813 oligo Seq

Sense Seq - CAGGAACAUCUCAGCCCUGAAUU

Anti-Sense Seq - UUCAGGGCUGAGAUGUUCCUGUU

hTBC1D9B 1039 oligo Seq

Sense Seq - AGGGAGGUGACCAUUGUCGAAUU

Anti-Sense Seq - UUCGACAAUGGUCACCUCCCUUU

RT PCR primers for TBC1D9B were purchased from BioRad Laboratories, USA. SYBR Green RT PCR mix was purchased from Applied Biosciences and DEPC treated water was purchased from Invitrogen (USA). 96 well RT PCR plates were purchased from Genaxy Scientific.

2.1.5 Cell Culture Reagents

Dulbecco's modified eagle medium (DMEM), Trypsin-EDTA 0.05%, DPBS, antibiotic–antimycotic mix, Polyethylenimine (PEI), fetal bovine serum (FBS), RNase free water, Opti-MEM media and most other cell culture reagents were obtained from Lonza Bioscience (USA) and Thermoscientific (USA). Dharmafect transfection reagent was purchased from DHARMACON and X-tremeGene HP DNA transfection reagent was purchased from Sigma Aldrich (USA). Paraformaldehyde (PFA) was purchased from Sigma Aldrich and Fluoromount-G™ aqueous mounting medium was purchased from Southern Biotech.

HEK293T cells used were from MBB lab and HeLa cells used were from NA lab.

2.1.6 Cell Culture Instruments

Cell culture hoods were from Labconco (USA), Confocal Microscope (Zeiss 710) was from Zeiss (Germany), tissue culture incubators were from NEB (USA), Eppendorf 5810R centrifuge was from Eppendorf (Germany), EasyPets were from Eppendorf, pipette aids were from Thermo Fisher Scientific (USA).

2.1.7 Plasticware and Chemicals

Plastic and glasswares for tissue culture studies were purchased from Thermo Scientific®; Falcon®, USA; Tarsons®, India; Fisher Scientific®, USA and BD Biosciences, USA. Bacterial media, agar, salts and chemicals were purchased from BD Difco, Himedia, Sigma Aldrich, Merck limited® and Thermo Scientific.

2.2 Methods

2.2.1 Preparation of Ultra-Competent *E. coli* DH5α cells

E. coli DH5α cells were streaked from a strain on a fresh Luria agar plate without antibiotics and incubated overnight at 37°C. A single colony was picked and inoculated in 5 mL LB medium overnight at 37°C. 1% of the primary culture was inoculated in 50mL of SOB and incubated at 37°C until the optical density of the culture reached 0.4 - 0.6. The culture was then incubated on ice for 10 mins and centrifuged for 10 mins at 3500rpm at 4°C. The supernatant was discarded and the pellet was resuspended gently by adding 25mL Transformation buffer #1. The suspension was incubated on ice for 10 mins and subsequently it was centrifuged at 3500 rpm at 4°C for 10 min. Supernatant was discarded and the pellet was resuspended in 4 ml of Transformation Buffer #2 and 140µL of DMSO was added thereafter. The suspension was incubated on ice for 15 mins and another 140µL of DMSO was added.

Aliquots of 100µL each were prepared in pre-chilled 1.5mL microcentrifuge tubes and stored immediately in -80°C. 20µL of the prepared competent cells were spread each on Amp, Kan or Strep plate to check for contamination.

For transformation of ligation, a 1:1 ratio of competent cells and transformation buffer #3 was used and the standard protocol was followed.

2.2.2 Transformation into *E. coli* cells

The *E. coli* competent cells were thawed on ice for 10 minutes. 100 ng DNA was added to 50µL cells and incubated on ice for 30 mins. Heat shock was given at 42°C for 90 seconds and the cells were transferred back on the ice for 5 mins. Subsequently, 1 mL LB media was added and the culture was incubated at 37°C for an hour. The cells were then centrifuged at 6000 rpm for 5 mins. The media was discarded and the pellet was resuspended in 100 µL LB media and plated on antibiotic-containing LB agar plates.

2.2.3 Plasmid Isolation

Isolation of plasmids for transfection purposes in cells was done using Thermo Scientific™ Gene JET Plasmid Miniprep kits according to the instruction manual.

2.2.4 Cloning

PCR amplification was done using the template and the primers for the required gene. The PCR was checked by running some amount of it on 0.8% Agarose gel.

The PCR product was then purified using Thermo Scientific™ Gene JET PCR purification kit. 2μg of the purified product was digested along with the vector. The digested product and vector were run on 1% nuclease-free agarose gel and suitable bands of the insert and vector were purified from the gel. Ligation was set up at 25°C for 3 hours using the vector and insert in the ratio of 1:3. The ligated product was transformed into DH5α cells as per protocol in 2.2.1 and 2.2.2. The colonies thus obtained were then screened for positive clones using the Phenol-chloroform-isopropyl alcohol screening method. The positive clones were verified by digesting their DNA and checking on gel. Finally, the positive clones were verified using sanger sequencing.

2.2.5 Purification of GST protein and GST Pulldown assay

pGEX4T3 vector containing GST and GST bound protein of interest were transformed into *E. coli* BL21 cells and primary culture was set up from the freshly transformed plate. One colony from each of the two was picked and incubated in 5mL LB media (with 5 μL Ampicillin) at 37°C for 8-10 hours. 50mL of superbroth media each (with salt solution) was taken and 1% inoculum from the primary culture was added to the respective flasks to set up the secondary culture. The secondary cultures were incubated at 37°C until the optical density reached 0.4-0.6 (approx. 2.5-3 hours). Induction with 0.5mM IPTG was given to the secondary cultures and they were kept for overnight incubation at 16°C for protein induction.

The secondary cultures were then centrifuged at 4000 rpm for 10 mins at 4°C. The supernatant was discarded carefully and the pellet was suspended in 5-10mL of Prep buffer on ice. Sonication of cells was done using ultrasound sonicator and the sonicated culture was then centrifuged at 10,000 rpm for 15 mins to separate the cell debris. The supernatant was carefully collected in a 15 mL falcon. Meanwhile, 50μL slurry of glutathione beads each was taken out in two 1.5mL MCT and 2-3 washes were given to the beads with Prep buffer. The beads were then transferred to the 15mL falcon containing protein soup for both GST only and GST bound protein, and it was kept on a Hula mixer at 4°C for 2-3 hours for the GST bound protein to bind to the glutathione beads.

After 3 hours, the beads were collected in a 1.5mL MCT by spinning down the sample at 1512 rpm at 4°C. Subsequently, 6-7 washes were given to the beads using

Prep buffer and the samples were prepared using 8 µL of bead slurry + 20µL of 2X reducing dye and heating it at 100°C for 10 mins. The samples were run on 10% SDS-Page gel until the dye front reached the end of the plate. The gel was then kept in Coomassie Blue staining solution overnight on the see-saw shaker. After overnight staining, the gel was put in the destaining solution for 4-6 hours on the see-saw shaker. Protein induced was quantified and the amount of slurry to be used for further experiment was decided to maintain similar protein levels.

The amount of beads taken in an MCT was such that the protein amount was sufficient enough for the experiment. 500 µL of 5% BSA prepared in 1X PBS was added to the MCTs and they were left for blocking on the Hula mixer for 3 hours at 4°C. Meanwhile, lysate of HEK293T cells (untransfected or transfected - as per the experiment) was prepared by collecting the cells in the TAP lysis buffer and leaving it on the Hula mixer for 30 mins at 4°C.

1% of the prepared lysate was saved as input and stored at -20°C after sample preparation. The rest of the lysate was divided equally in the MCTs with beads and the beads were left on the Hula mixer for 3 hours at 4°C. After pull-down, each of the samples was given 4 washes with TAP lysis buffer. The samples were prepared by adding 2X loading dye and heating at 100°C for 10 mins. The samples were run on 10% SDS-Page gel until the dye front reached the end of the plate. Semidry transfer was setup at 10V for 2 hours using the PVDF membrane. The membrane after transfer was put in 10% skimmed milk for 2 hours on see-saw shaker.

After blocking, 3 washes with 0.05% PBST of 10 mins each were given to the membrane on the dancing shaker. The primary antibody solution was then added to the membrane and it was kept on see-saw shaker for 3 hours. After incubation with primary antibody, 3 washes with 0.05% PBST of 10 mins each were given. The secondary antibody mix was added thereafter and the membrane was kept on see-saw shaker for 45 mins. After this, 3 washes with 0.3% PBST of 10 mins each were given to the membrane. The blot was finally developed in the darkroom using Amersham™ ECL™ Western Blotting Detection kit as per the protocol.

2.2.6 RNA Isolation and cDNA Synthesis

Isolation of RNA from cells was done using Qiagen® RNeasy mini kit as per the given protocol and subsequent cDNA synthesis was done using Invitrogen SuperScript™ III cDNA synthesis kit according to the manual.

2.2.7 RT PCR setup and Analysis

The reactions were prepared in the sets of three for getting triplicate readings. 0.6μL of RT PCR primers (0.3μL forward and 0.3μL reverse) for the gene were mixed with 5μL of SYBR Green RT PCR mix, 1μL of the synthesized cDNA and 3.4μL of DEPC treated water in each well for the set of three in Axygen 96 well RT PCR plate. For control triplicate, primers were not added and the volume was compensated using DEPC treated water. The PCR plate was given a short spin to settle down the reaction mix. The qPCR was set up in Eppendorf realplex⁴ qPCR machine.

Analysis of the qPCR data was done in MS Excel.

2.2.8 Cell culture - Transfection and siRNA Knockdown

2.2.8.1 <u>HEK cells Transfection:-</u> HEK293T cells were cultured in Dulbecco's modified eagle medium (DMEM) supplemented with 10% fetal bovine serum and antibiotic–antimycotic mix (1X) at 37°C and 5% CO_2. Cells were grown to a confluence of 65-70% on 60mm dishes. Transfection mix per well contained 1 μg of DNA and PEI in three times the volume of the DNA. Cells were then cultured with the transfection mix and 10% DMEM complete media and the constructs were allowed to express for 20-24 hours before performing experiments.

2.2.8.2 <u>HeLa cells Transfection:-</u> HeLa cells were cultured in Dulbecco's modified eagle medium (DMEM) supplemented with 10% fetal bovine serum and antibiotic–antimycotic mix (1X) at 37°C, 95% humidity and 5% CO_2. 0.18 million cells were seeded on coverslips placed in a 35mm dish. After 20-24 hours of seeding the cells, the coverslips were transferred in the wells of a 24 well plate containing 10% DMEM complete media. Transfection mix was prepared containing 50μL of Opti-MEM and 1:1 ratio of the amount of DNA (μg) and the volume (μL) of XtremeGene HP

transfection reagent. After mixing the components well, the transfection mix was allowed to incubate at room temperature for 30 mins. Transfection mix was then poured dropwise onto the coverslips in the well and the contents of the wells were mixed by moving the plate vertically and horizontally. The transfected coverslips were incubated at 37C and 5% CO_2 for 12-16 hours before performing further experiments.

2.2.8.3 <u>HeLa cells siRNA Knockdowns:-</u> HeLa cells were cultured in Dulbecco's modified eagle medium (DMEM) supplemented with 10% fetal bovine serum and antibiotic–antimycotic mix (1X) at 37C, 95% humidity and 5% CO_2. 0.06 million cells were seeded on coverslips placed in a 35mm dish. After 20-24 hours of seeding the cells, siRNA knockdown was performed. For control knockdown, scrambled siRNA was used. Two sets of MCTs for both control and experiment were prepared. For each control coverslip, set A consisted of (25µL opti-MEM + 24µL RNase free water + 1µL control siRNA) whereas Set B had (49µL opti-MEM + 1µL Dharmafect). Similarly, Set A and B for 'experiment' were made with the only change being that 2µL of siRNA was used. These were incubated for 10-15 mins at room temperature and then respective Set B was added to Set A and mixed thoroughly. The mixture was incubated at room temperature for 30 mins and poured dropwise onto the respective coverslips. Contents of the wells were mixed well and the transfected coverslips were incubated at 37C and 5% CO_2 for 60 hours before performing further experiments.

2.2.9   Immunostaining of HeLa cells

Cells grown on coverslips that were used for transfection or knockdown were first fixed in 4% PFA in PHEM buffer (60mM PIPES, 10mM EGTA, 25mM HEPES and 2mM $MgCl_2$ and final pH 6.8) for 10min at room temperature. Post-fixation, cells were incubated with the blocking solution (0.2% saponin + 5% FBS in PHEM buffer) at room temperature for 30mins, followed by three washes with 1X PBS. Following this blocking step, cells were incubated with primary antibodies in staining solution(PHEM buffer + 0.2% saponin) for 2 hours at room temperature. The coverslips were then given three washes with 1X PBS. Further, the coverslips with cells were incubated for 30-45 mins with Alexa fluorophore-conjugated

secondary antibodies made in staining solution. The coverslips were given three washes with 1X PBS and the cells were mounted in Fluoromount-G (Southern Biotech) on a slide. Finally, the confocal images were acquired using Carl Zeiss 710Confocal Laser Scanning Microscope.

2.2.10 Confocal Imaging and Analysis

Images were captured by Zeiss LSM 710 confocal laser scanning microscope using 63X oil immersion objective. Digital gain, digital offset, laser power and all other parameters were set as per experimental controls and were preserved throughout the experiment. ImageJ, an open-source software (NIH, USA) was used to analyze all images. Final processing of images was done using Adobe Photoshop.

Chapter 3
Results

**TBC1D9B, a TBC domain-containing protein interacts with Arl8b**

To discover novel interaction partners of Arl8b, the approach of pull-down assays followed by mass spectrometric analysis was employed. GST-Arl8b was incubated with HEK293T cell lysate and mass spectrometry was performed previously in the lab (data not shown). Mass spectrometry results showed TBC1D9B protein as a possible positive hit and thus we hypothesized it to be an interaction partner of Arl8b.

Myc tagged TBC1D9B construct was made by incorporating myc tag at the N terminus of full-length TBC1D9B protein. GST pull-down assays were performed using GST-Arl8b WT bound on glutathione beads and incubating with cell lysate of HEK293T cells expressing myc tagged TBC1D9B. Two independent experiments were performed and our findings suggest that TBC1D9B interacts with Arl8b in GST pull-down assays.
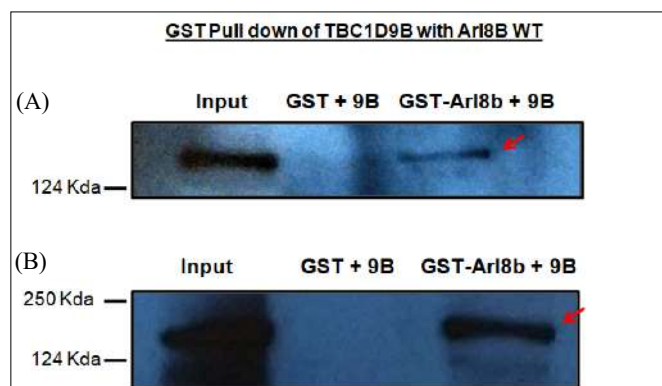
Figure 3.1.1: GST Pulldown assays were done using GST-Arl8b WT and lysate from HEK 293T cells transfected with myc tagged TBC1D9B. 6μg of myc tagged TBC1D9B DNA was used for transfection per 60mm dish of HEK293T cells. Since TBC1D9B has transfection issues, DNA isolated from freshly transformed *E. coli* cells was used. Two independent experiments were performed and for both (A) and (B), 1% lysate was saved and run as input. Only GST bound to glutathione beads was used as negative control. Samples were resolved on SDS-Page gel and semi-dry gel transfer settings were kept the same for both the experiments. The blot was probed using anti-myc mouse antibody (SCBT). HRP-conjugated goat anti-mouse antibody was used as secondary and the blot was developed using Amersham ECL kit in darkroom. TBC1D9B band was seen at around 140 kDa in both the experiments. Band of TBC1D9B in expt. (B) was stronger as more amount of cell lysate was used.
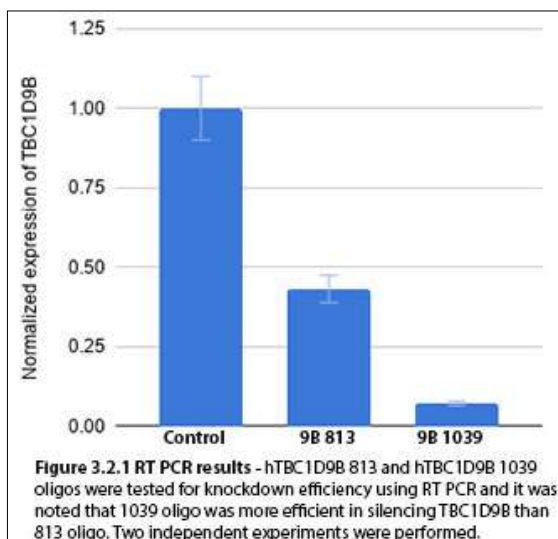
Further, we were intrigued to find out sub-cellular localization of TBC1D9B; however, we observed that it is majorly cytosolic (Figure 3.1.2) when myc tagged TBC1D9B is expressed in HeLa cells. Since no working antibody for TBC1D9B was available, determining its sub-cellular localization was not possible. Interestingly, when myc tagged TBC1D9B was co-transfected with Arl8b tagged with HA in HeLa cells, some weak co-localization was seen at the tips of the cells (Figure 3.1.2).
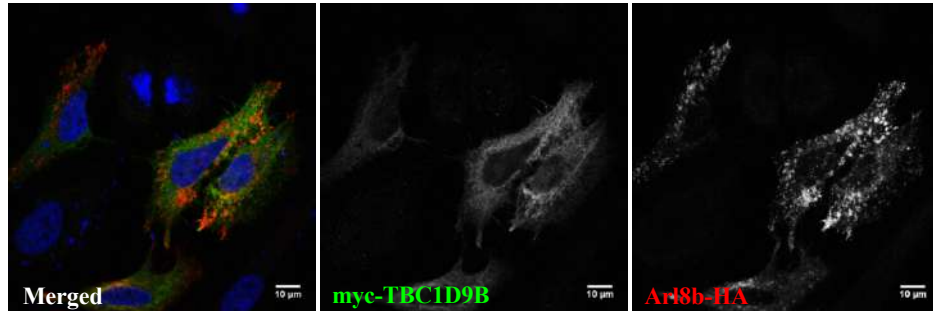

Figure 3.1.2 Weak localization of myc tagged TBC1D9B at the cell tips. 1µg DNA of myc tagged TBC1D9B and 0.3µg DNA of Arl8b tagged with HA were transfected into HeLa cells. Immunostaining was done with anti-myc mouse antibody and anti-HA rabbit antibody. Three independent experiments were performed. Images were analyzed offline after acquisition using ImageJ and processing was done using Adobe Photoshop.

3.2 Late endosomal/lysosomal structures are affected upon TBC1D9B depletion, but autophagosomes seemed to be unaffected.

To determine the cellular roles of TBC1D9B, we took an unbiased approach of looking at different cellular compartments upon the knockdown of TBC1D9B. We used well-known markers for various intracellular compartments (Figure 3.2.2) and looked for changes upon TBC1D9B depletion.

Figure 3.2.1 RT PCR results - hTBC1D9B 813 and hTBC1D9B 1039 oligos were tested for knockdown efficiency using RT PCR and it was noted that 1039 oligo was more efficient in silencing TBC1D9B than 813 oligo. Two independent experiments were performed.

For RNAi depletion, we used two different siRNAs (Section 2.1.4) and tested their efficiency by doing RT PCR (Figure 3.2.1). hTBC1D9B 813 oligo showed around 70% knockdown efficiency while hTBC1D9B 1039 oligo had more than 90% knockdown efficiency. All the experiments were performed using both the knockdown siRNA oligos to assess whether the phenotype is observed with both oligos.

19
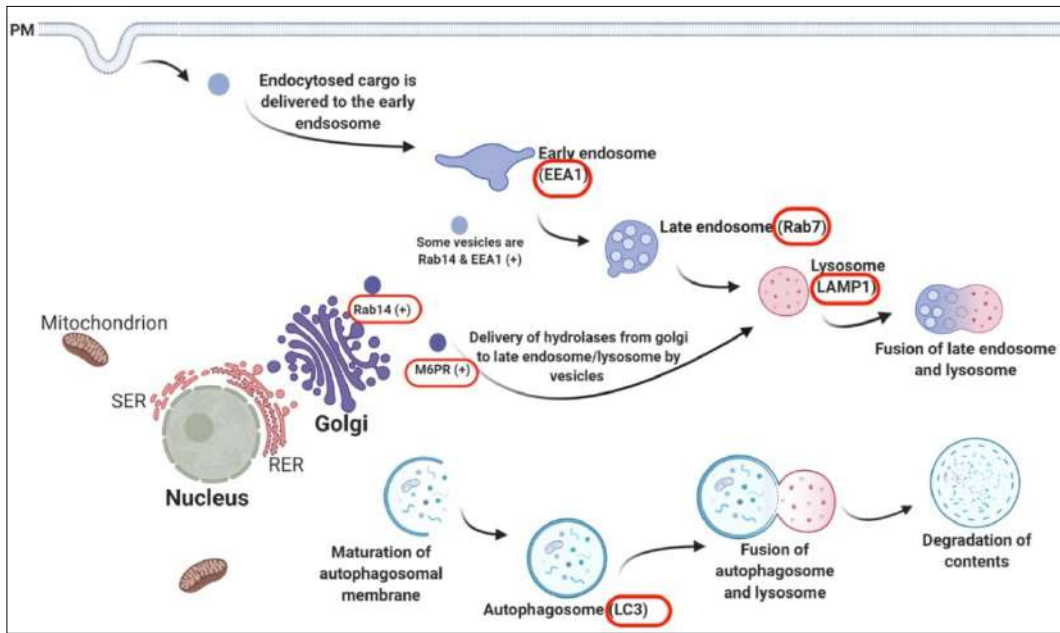
Figure 3.2.2 Intracellular Trafficking. Markers used for immunostaining upon TBC1D9B depletion are highlighted in red colour. Image prepared using BioRender.

To begin with, we chose to check LAMP1 compartments upon TBC1D9B depletion. We had already established that TBC1D9B interacts with Arl8b (Section 3.1) and Arl8b is a crucial regulator of lysosome motility and functioning. Thus, looking at LAMP1 (+) compartments in the background of TBC1D9B depletion was the obvious next step.

20
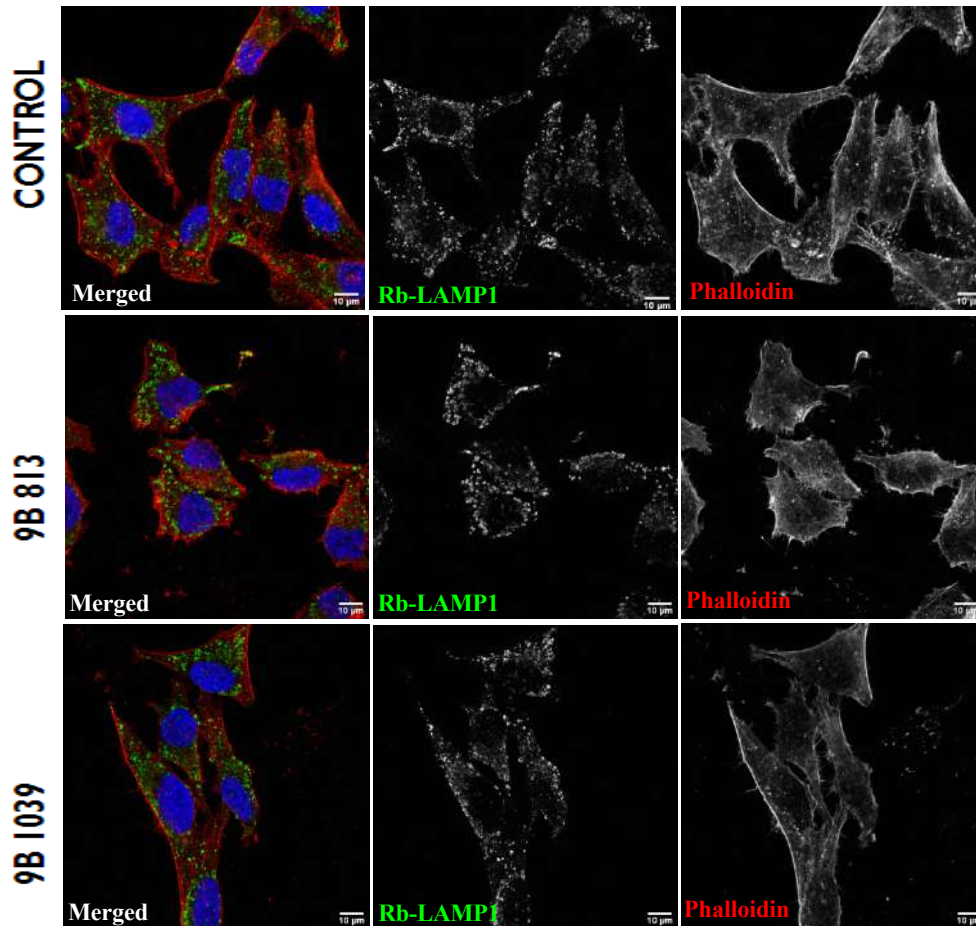
Figure 3.2.3 LAMP1 (+) compartments are enlarged in TBC1D9B knockdown.
(A) siRNA knockdown in HeLa cells was done as per 2.2.8.3 and anti-LAMP1 rabbit antibody (abcam) was used along with phalloidin (to get an idea of the shape of the cell). Analysis of images was done using ImageJ and the final processing was done using Adobe photoshop.

The experiments showed that upon TBC1D9B depletion, LAMP1 (+) structures are enlarged significantly (Figure 3.2.1). Besides the change in size, some cells even showed few changes in the distribution of LAMP1 compartments. The LAMP1 structures in some cells appeared to be positioned in the perinuclear region along with the phenotype of size enlargement. Since LAMP1 is a lysosomal associated membrane protein, some LAMP1 (+) structures appeared as rings due to size enlargement. LAMP1 particle size was quantified over two experiments (n ≥50) (Figure 3.2.2) using ImageJ. These findings suggest that LAMP1 particle size and LAMP1 integrated density (area x mean intensity) both are increased upon TBC1D9B depletion. Also, the number of LAMP1 compartments was observed to be less in knockdown cells. Surprisingly, knockdown with 813 oligo (~70% KD) showed more dramatic effects as compared to with 1039 oligo (>90% KD). This trend was observed with some other markers too. Thus, we speculate that maybe partial knockdown of TBC1D9B affects the cell more or maybe upon >90% knockdown of TBC1D9B, some compensatory pathway is activated involving it's paralogue TBC1D9A. All these speculations need further experimentation to be verified.
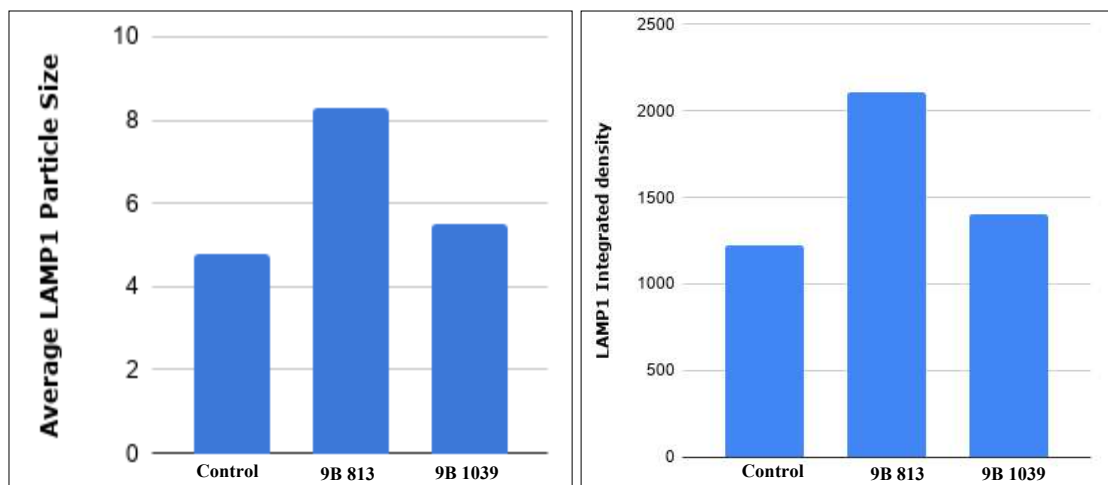
Figure 3.2.4 Quantification of LAMP1 particle size and intensity. ImageJ was used to quantify the data for particle size and intensity. Cells were individually selected and threshold was set using Otsu algorithm. Integrated density, Average particle size and intensity were calculated using the 'Analyze Particles' tool in ImageJ.

To further determine other endosomal compartments affected by TBC1D9B knockdown, we looked at late endosomal compartments. Although late endosomes are of different forms with distinct cisternal, tubular and multivesicular regions, they are mainly considered to the multivesicular bodies that act as key sorting hubs and are responsible for sorting and delivery of vesicular contents to the lysosomes. We chose Rab7 GTPase present on the late endosomal membrane as a marker to visualize late endosomes in TBC1D9B depletion conditions.
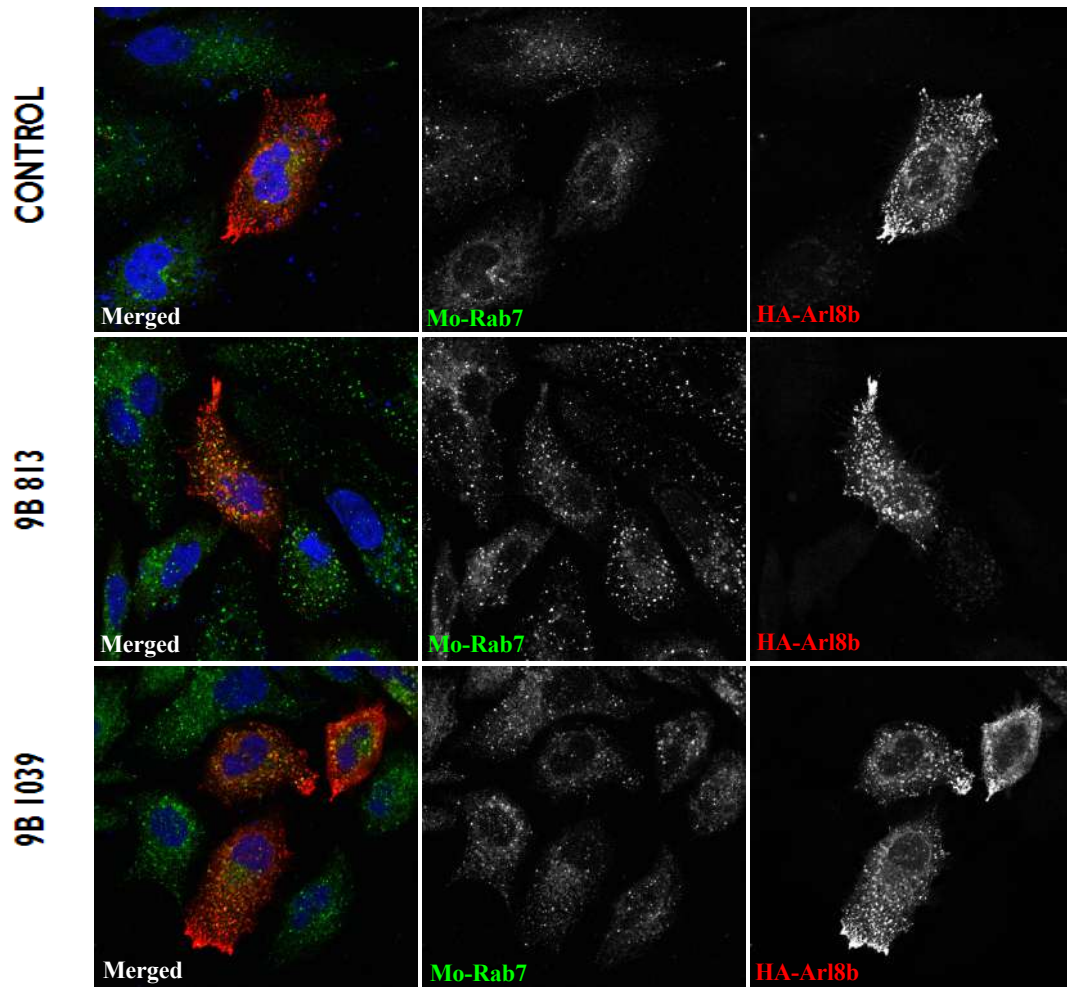
Figure 3.2.5 Rab7(+) compartments are enlarged upon TBC1D9B knockdown. siRNA knockdown in HeLa cells was done as per 2.2.8.3. 0.3 µg DNA of HA-tagged Arl8b was transfected each into control and knockdown cells 48 hours after siRNA knockdown and 12 hours transfection period is given before the experiment. Anti-rab7 mouse and anti-HA rabbit antibodies were used for immunostaining. Image acquiring parameters were kept the same for all the images. Analysis of images was done using ImageJ and final processing was done using Adobe Photoshop.

We observed that Rab7 (+) compartments are enlarged in TBC1D9B knockdown cells (Figure 3.2.5). The late endosomes appear to be bigger and brighter in staining as

compared to control cells. The number of late endosomes also seemed to have increased in some of the knockdown cells. The change in intensity of Rab7 signal was quantified for one experiment with n=40 cells and we noted that the intensity of Rab7 signal increased in TBC1D9B knockdown cells (Figure 3.2.6).
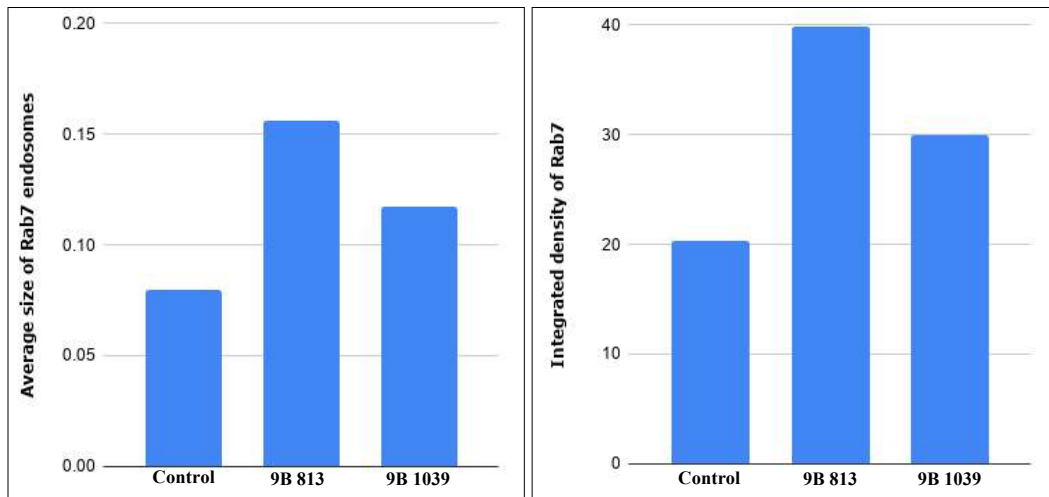

Figure 3.2.6 Quantification of Rab7 size and intensity. ImageJ was used to quantify the data. Threshold-ing was done using Otsu algorithm and integrated density particle size ofRab7 endosomes were calculated using the 'Analyze particles' tool in ImageJ. Final plots were prepared in MS excel using the average values.

A change in average size of Rab7 endosomes in knockdown cells was noted upon quantification. The change in intensity of Rab7 signal was also dramatic in TBC1D9b depleted cells. However, the changes were more dramatic with hTBC1D9B 813 oligo than 1039 oligo. Further experiments and independent repeats are needed to determine the causes of the defects observed in Rab7 endosomes upon TBC1D9B depletion.

Our findings till now suggested that late endosomes and lysosomes were affected in TBC1D9B knockdown. Autophagosome formation is a key step in the autophagic pathway which is marked by the recruitment of LC3 on the autophagosomal membrane. One published report (Liao et al 2018) already shows that TBC1D9B interacts with LC3B and positively regulates autophagic flux. Thus, to check the effect on TBC1D9B depletion on autophagosomes, we used LC3 as a marker and checked whether autophagosomes were affected or not.
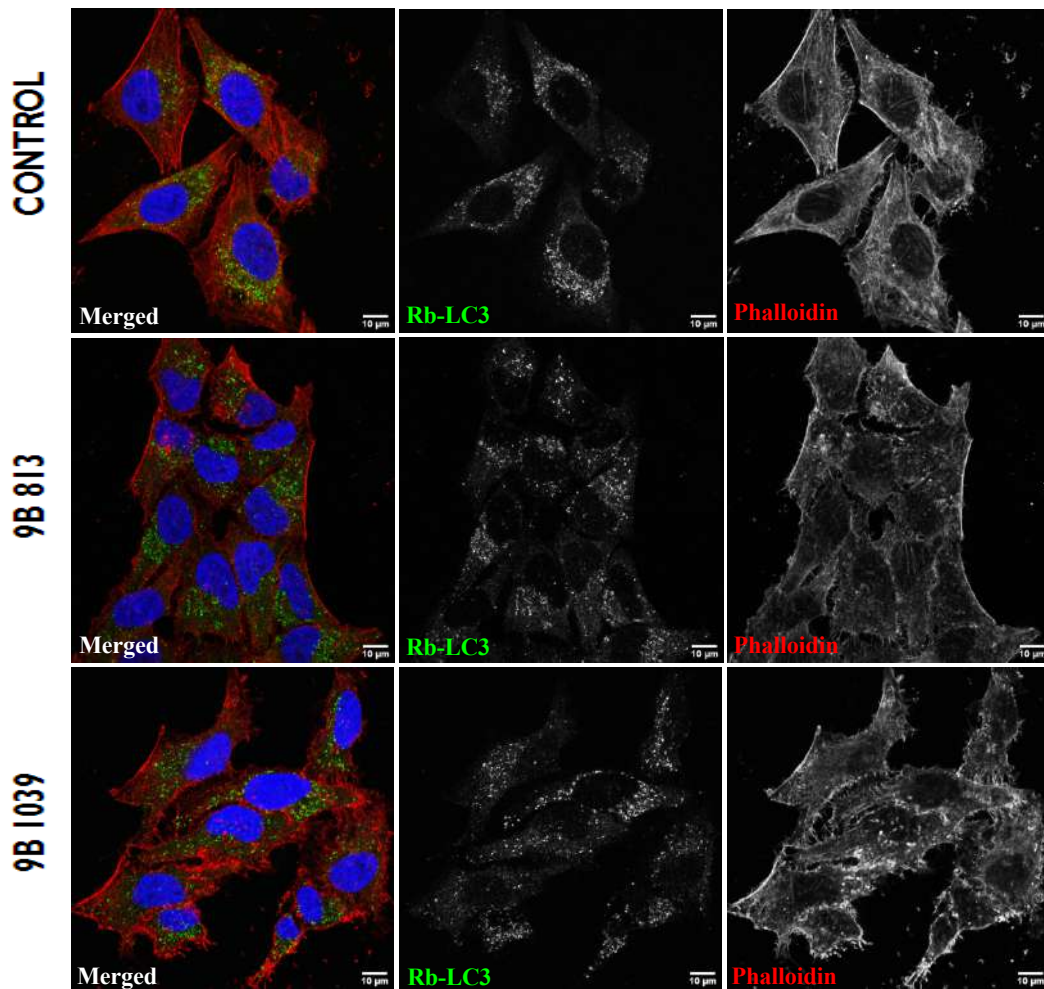
Figure 3.2.7 LC3 structures seemed to be unaffected in TBC1D9B knockdown.
siRNA knockdown in HeLa cells was done as per 2.2.8.3 and polyclonal antibody against
LC3 was used to stain autophagosomes. Analysis was done using ImageJ processing was
done using Adobe Photoshop.

Visibly, we found that autophagosomes were not significantly affected in TBC1D9B
knockdown conditions (Figure 3.2.7). The size and distribution of autophagosomes in
TBC1D9B knockdown cells was similar to control cells. However, due to numerous LC3
punctae in the cell, it is difficult to assess visually whether there was a modest change in
the number of LC3 punctae. This experiment was performed once and thus these
observations are preliminary. More independent repeats are needed to derive conclusions.

3.3 Endosomal structures other than late endosomes are also affected upon TBC1D9B depletion

To further investigate the vesicles that were affected by TBC1D9B knockdown, we
decided to look upon endosomal compartments. Rab14 is a GTPase that is known to
localize on early/recycling endosomes. It is also known to be on rough endoplasmic

reticulum and trans-Golgi network. Nonetheless it is usually considered as a good marker for early endosomes and recycling endosomes. Thus, we used Rab14 GTPase as a marker and looked at early/recycling endosomal structures.
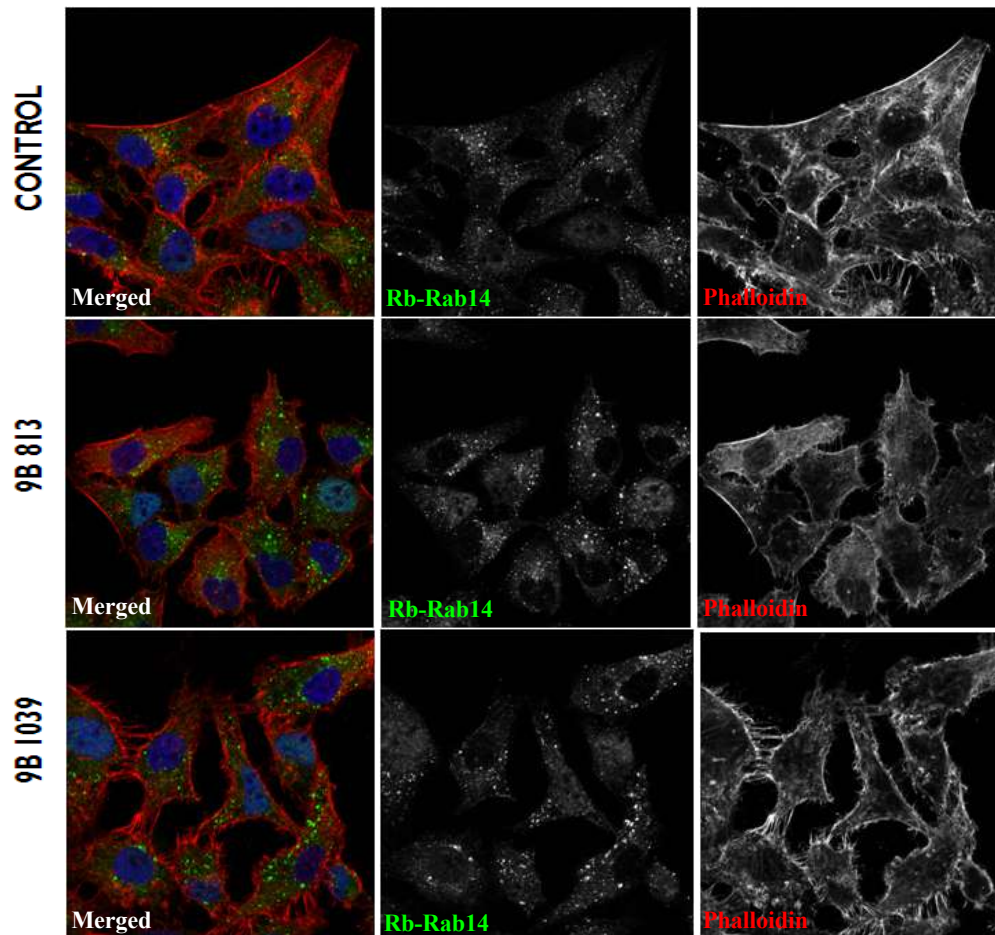
Figure 3.3.1 Rab14 (+) structures are enlarged upon TBC1D9b knockdown. siRNA knockdown in HeLa cells was done as per 2.2.8.3. Anti-rab14 rabbit antibody was used for immunostaining. ImageJ was used for analysis and Adobe Photoshop for processing.

At least 50 cells were imaged and analyzed and the confocal images represented that Rab14 (+) structures were enlarged in TBC1D9B knockdown. Most of the knockdown cells showed that Rab14 structures were larger than in control cells. From this observation, we can speculate that TBC1D9B might be acting as a GAP for Rab14 and its depletion is leading to less of membrane-bound Rab14-GTP being converted into Rab14-GDP form. Further investigations are needed to confirm this hypothesis.

We next used EEA1 as a marker to visualize early endosomes upon TBC1D9B depletion. EEA1 (Early endosome antigen 1) is known to localize exclusively to early endosomes. It is a membrane-bound effector of Rab5 and plays a crucial role in membrane trafficking. Thus, we used EEA1 to look at early endosomes upon TBC1D9B knockdown.
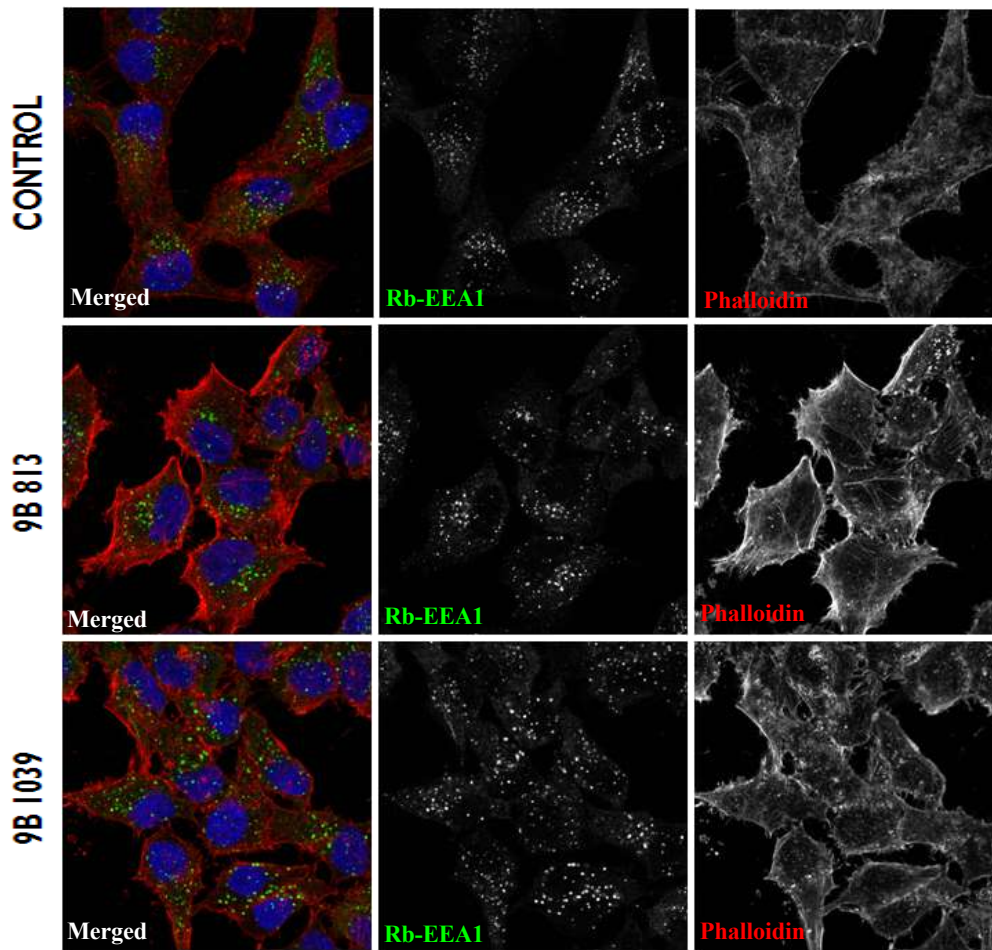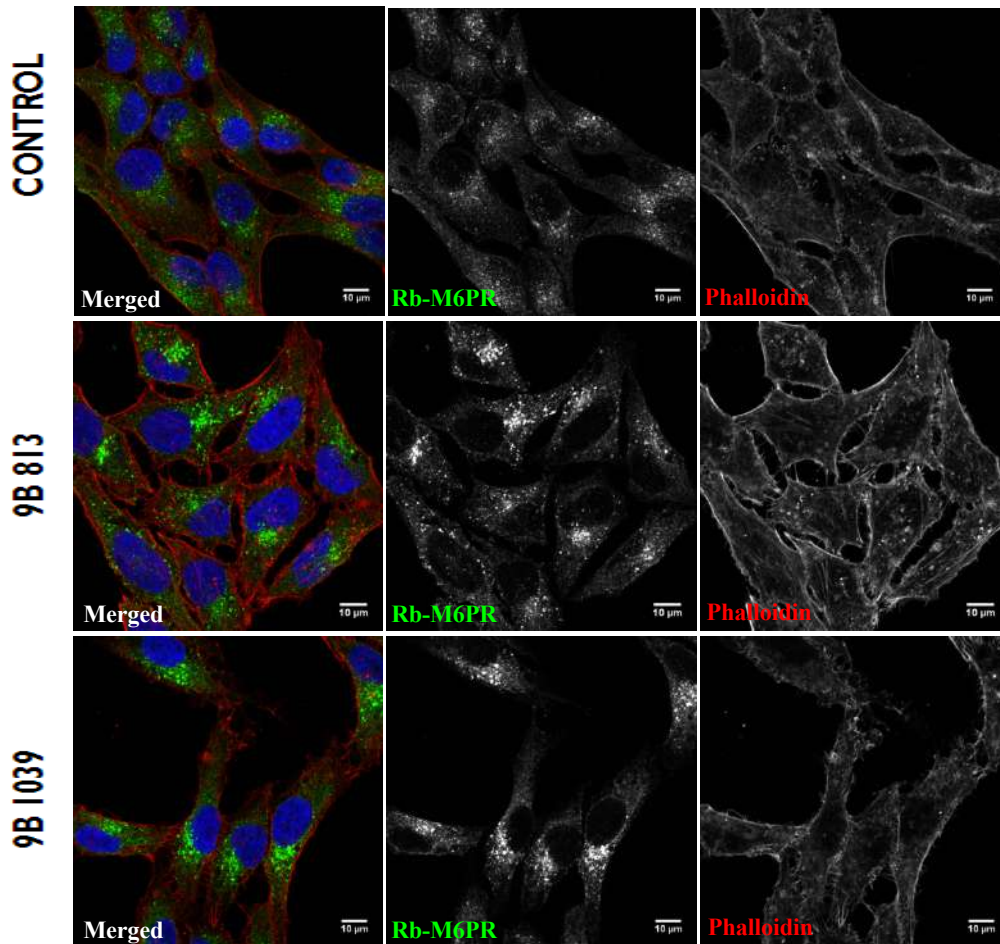
Figure 3.3.2 Some EEA1 puncta are enlarged upon TBC1D9B knockdown. siRNA knockdown in HeLa cells was done as per 2.2.8.3 and anti-EEA1 antibody was used in for immunostaining. Image acquiring parameters were kept the same for all the images. Analysis of images was done using ImageJ and final processing was done using Adobe Photoshop.

At least 50 cells were imaged and we found that not all EEA1 (+) compartments were affected by TBC1D9B knockdown (Figure 3.3.2). Still many puncta in the knockdown cells appeared enlarged as compared to the control cells. EEA1 could act as a bridge for the fusion of two membrane vesicles that bear Rab5. Thus, some increase in EEA1 might suggest that there is more homotypic fusion of Rab5 compartments. Further detailed investigation is needed to determine the reasons for the change in EEA1 staining.

Next we decided to check Mannose-6-phosphate receptor (M6PR)staining upon TBC1D9B depletion. M6PRs are transmembrane receptors responsible for binding the newly synthesized enzymes in the trans-Golgi network and transport them to the lysosomes. M6PRs are essential for the delivery of hydrolases that are responsible for the

degradation of lysosomal contents. Rab14 compartments are one of the vesicles that carry M6PRs and since Rab14 (+) compartments were enlarged in TBC1D9B knockdown (Figure 3.3.1), we thought of looking at M6PR staining in TBC1D9B knockdown cells.
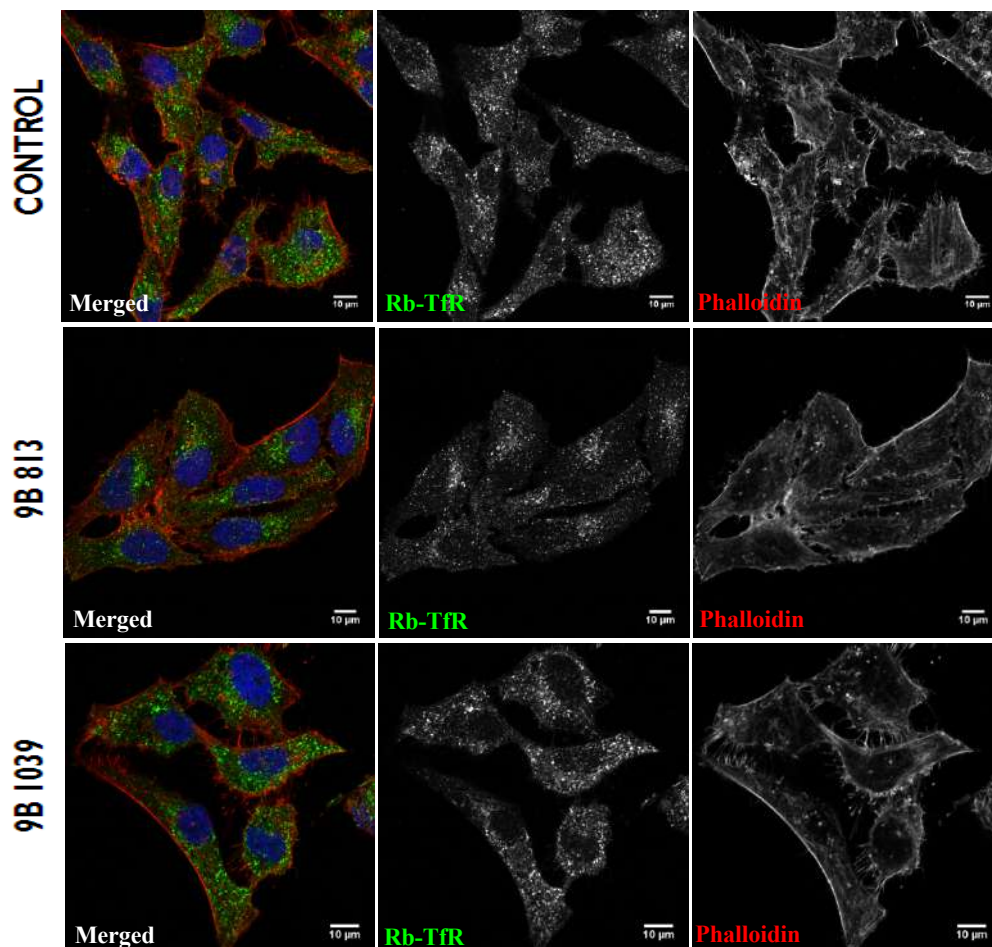

Figure 3.3.3 M6PR staining is enhanced upon TBC1D9B knockdown. siRNA knockdown in HeLa cells was done as per 2.2.8.3 and anti-M6PR rabbit antibody was used for immunostaining. Image acquiring parameters were kept the same for all the images. Analysis of images was done using ImageJ.

We found that in TBC1D9B knockdown cells, M6PR staining is significantly enhanced as compared to the control cells. M6PR usually can be on the same compartment as Rab14. Increase in Rab14 compartment size (Figure 3.3.1) as well as enhanced M6PR staining can suggest that a defect in the delivery pathway of lysosomal hydrolases from Golgi to lysosomes. Such hypotheses need to be tested to derive conclusive observations.

3.4 Transferrin receptor was similar in control and upon TBC1D9B knockdown

We next assessed the distribution of transferrin receptor (TfR) that marks the recycling endosomes. TfR is expressed on the membrane surface of the cell and is responsible for the import of iron by forming a transferrin-iron complex that is endocytosed. Once the receptor is internalized, iron is dissociated from the transferrin-receptor complex and both transferrin and the receptor undergo slow recycling from the endocytic recycling compartment to the plasma membrane (Donaldson & Grant et al., 2009).We stained and observed the Transferrin receptor in TBC1D9B knockdown conditions.

Figure 3.4TfR is unaffected in TBC1D9B knockdown. siRNA knockdown in HeLa cells was done as per 2.2.8.3 and anti-TfR rabbit antibody was used for immunostaining. Image acquiring parameters were kept the same for all the images. Analysis of images was done using ImageJ and final processing was done using Adobe Photoshop.

At least 50 cells were imaged and we observed that the Transferrin receptor staining was not affected in TBC1D9B knockdown. The TfR staining was similar in both control and knockdown cells. Again, it is to be noted that this experiment was done once and thus these findings are preliminary and need to be reconfirmed with independent experiments.

Chapter 4

Conclusion and Future Directions

In summary, our findings present TBC1D9B as a novel interaction partner of Arl8b. Establishing the significance of this interaction and the regions in TBC1D9B and Arl8b responsible for this interaction is the goal of our future experiments. Also, the function of different domains of TBC1D9B needs to be investigated. Further, we report that human TBC1D9B has homologs in other established model systems as well. Upon knockdown of TBC1D9B, we observed several changes in various intracellular organelles and membrane vesicles. LAMP1(+) compartments were enlarged upon TBC1D9B depletion, which could be due to many reasons including homotypic fusion of LAMP1 structures or impaired degradation of lysosomal contents. Further investigation is needed to establish the exact cause of the enlargement of LAMP1 compartments. Besides this, we also observed larger and brighter endosomes positive for Rab7 and Rab14 upon TBC1D9B depletion. We also observed enlarged EEA1 compartments and enhanced staining for M6PR upon TBC1D9B knockdown.

The changes observed in Rab14 and Rab7 structures upon TBC1D9B knockdown can be an interesting finding to pursue. Previous studies have established that one TBC protein can act as GAP for multiple Rabs in the cell (Itoh et al., 2006). Thus, we speculate that Rab7 or Rab14 might both act as Rab substrates for TBC1D9B. Another possibility can be that hyperactivation of one Rab affects the other compartments. For instance, constitutive activation of Rab7 can affect the upstream endosomal compartments including EEA1/Rab14 compartments. That may be one of the reasons why EEA1 and Rab14 compartments are affected upon TBC1D9B depletion. Recent reports also suggest Rab2A as a potential substrate for TBC1D9B. Further investigations are needed to establish the Rab substrate of TBC1D9B. Besides this, TBC1D9B also has a paralogue, TBC1D9A, which also interacts with Arl8b according to our preliminary investigations (unpublished work by Shalini Rawat). As part of future studies, we are keenly interested in deciphering the cellular roles of TBC1D9A and TBC1D9B, identity of their Rab substrates and their roles in regulating cargo transport and degradation.

Bibliography

1. Gruenberg, Jean. "The Endocytic Pathway: a Mosaic of Domains." *Nature Reviews Molecular Cell Biology*, vol. 2, no. 10, 2001, pp. 721–730., doi:10.1038/35096054.

2. Song, Siyang, et al. Small GTPases: Structure, Biological Small GTPases: Structure, Biological Function and Its Interaction with Nanoparticles." *Asian Journal of Pharmaceutical Sciences*, vol. 14, no. 1, 2019, pp. 30–39., doi:10.1016/j.ajps.2018.06.004.

3. Zhen, Y., & Stenmark, H. (2015). Cellular functions of Rab GTPases at a glance. *Journal of cell science*, *128*(17), 3171-3176. doi.org/10.1242/jcs.166074.

4. Nielsen, Erik, et al. "The Regulatory RAB and ARF GTPases for Vesicular Trafficking." *Plant Physiology*, vol. 147, no. 4, 2008, pp. 1516–1526. *JSTOR*, www.jstor.org/stable/40066093. Accessed 1 May 2020.

5. Donaldson JG, Jackson CL. ARF family G proteins and their regulators: roles in membrane transport, development and disease. Nat Rev Mol Cell Biol 2011; 12:362-75; PMID:21587297; http://dx.doi.org/ 10.1038/nrm3117.

6. Pu J, Schindler C, Jia R, Jarnik M, Backlund P, Bonifacino JS. BORC, a multi subunit complex that regulates lysosome positioning. Dev Cell 2015; 33:176-88; PMID:25898167; http://dx.doi.org/10.1016/j. devcel.2015.02.011.

7. Hofmann I, Munro S. An N-terminally acetylated Arflike GTPase is localised to lysosomes and affects their motility. J Cell Sci 2006; 119:1494-503; PMID:16537643; dx.doi.org/10.1242/jcs.02958.

8. Divya Khatter, Vivek B. Raina, Devashish Dwivedi, Aastha Sindhwani, Surbhi Bahl, Mahak Sharma. Journal of Cell Science (2015) 128: 1746-1761; doi: 10.1242/jcs.162651.

9. Rik van der Kant, Alexander Fish, Lennert Janssen, Hans Janssen, Sabine Krom, Nataschja Ho, ThijnBrummelkamp, Jan Carette, Nuno Rocha, Jacques Neefjes Journal of Cell Science (2013) 126: 3462-3474; doi: 10.1242/jcs.129270.

10. Lőrincz, P., & Juhász, G. (2019). Autophagosome-lysosome fusion. Journal of Molecular Biology. doi:10.1016/j.jmb.2019.10.028

11. Bright NA, Reaves BJ, Mullock BM, Luzio JP. Dense core lysosomes can fuse with late endosomes and are reformed from the resultant hybrid organelles. J Cell Sci. 1997;110:2027–2040.

12. Richardson, P. M. and Zon, L. I. Molecular cloning of a cDNA with a novel domain present in the tre-2 oncogene and the yeast cell cycle regulators BUB2 and cdc16.

Oncogene 11, (1995).

13. Pan, X., Eathiraj, S., Munson, M. and Lambright, D. G. (2006) TBC-domain GAPs for Rab GTPases accelerate GTP hydrolysis by adual-finger mechanism. Nature 442, 303–306.

14. Gavriljuk, K., Gazdag, E.-M., Itzen, A., Kotting, C., Goody, R. S., & Gerwert, K. (2012). *Catalytic mechanism of a mammalian Rab-Rab GAP complex in atomic detail. Proceedings of the National Academy of Sciences, 109(52), 21348–21353.* doi:10.1073/pnas.1214431110.

15. Doerks, T., Strauss, M., Brendel, M., & Bork, P. (2000). *GRAM, a novel domain in glucosyltransferases, myotubularins and other putative membrane-associated proteins. Trends in Biochemical Sciences, 25(10), 483–485.*

16. Frasa MA, Koessmeier KT, Ahmadian MR, Braga VM (2012). Illuminating the functional and structural repertoire of human TBC/RABGAPs. Nat Rev. Mol Cell Biol 13, 67-73.

17. Gabernet-Castello, Carme, et al. "Evolution of Tre-2/Bub2/Cdc16 (TBC) Rab GTPase-Activating Proteins." *Molecular Biology of the Cell*, vol. 24, no. 10, 2013, doi:10.1091/mbc.e12-07-0557.

18. Itoh, T., Satoh, M., Kanno, E. and Fukuda, M. (2006) Screening for target Rabs of TBC (Tre-2/Bub2/Cdc16) domain-containing proteins based on their Rab-binding activity.GenesCells11,1023–1037.

19. Nozawa, T., Okamoto-Furuta, K., Kohda, H. & Nakagawa, I. Rab35 GTPase recruits NDP52 to autophagy targets. *EMBO J.* **36**, 2790–2807 (2017).

20. Itoh, T., Kanno, E., Uemura, T., Waguri, S. & Fukuda, M. OATL1, a novel autophagosome-resident Rab33B-GAP, regulates autophagosomal maturation. *J. Cell Biol.* **192**, 839–853 (2011).

21. Popovic, D. et al. Rab GTPase-activating proteins in autophagy: regulation of endocytic and autophagy pathways by direct binding to human ATG8 modifiers. *Mol. Cell. Biol.* **32**, 1733–1744 (2012).

22. Longatti, A. et al. TBC1D14 regulates autophagosome formation via Rab11- and ULK1-positive recycling endosomes. *J. Cell Biol.* **197**, 659–675 (2012).

23. Yamano, K., Fogel, A. I., Wang, C., van der Bliek, A. M. & Youle, R. J. Mitochondrial Rab GAPs govern autophagosome biogenesis during mitophagy. *eLife* **3**, e01612 (2014).

24. Baba, T., Toth, D. J., Sengupta, N., Kim, Y. J., & Balla, T.

(2019). *Phosphatidylinositol 4,5-bisphosphate controls Rab7 and PLEKMH1 membrane cycling during autophagosome–lysosome fusion. The EMBO Journal, e100312.* doi:10.15252/embj.2018100312.

25. Gallo, L. I., Liao, Y., Ruiz, W. G., Clayton, D. R., Li, M., Liu, Y.-J., Yin, X.-M. (2014). *TBC1D9B functions as a GTPase-activating protein for Rab11a in polarized MDCK cells. Molecular Biology of the Cell, 25(23), 3779–3797.* doi:10.1091/mbc.e13-10-0604.

26. Liao, Y., Li, M., Chen, X., Jiang, Y., & Yin, X.-M. (2018). *Interaction of TBC1D9B with Mammalian ATG8 Homologues Regulates Autophagic Flux. Scientific Reports, 8(1).* doi:10.1038/s41598-018-32003-2.

27. Nozawa, T., Sano, S., Minowa-Nozawa, A. *et al.* TBC1D9 regulates TBK1 activation through Ca^{2+} signaling in selective autophagy. *Nat Commun* **11,** 770 (2020). https://doi.org/10.1038/s41467-020-14533-4.

28. Andres, S. A., Smolenkova, I. A., &Wittliff, J. L. (2014). *Gender-associated expression of tumor markers and a small gene set in breast carcinoma. The Breast, 23(3), 226–233.* doi:10.1016/j.breast.2014.02.007.

29. Junutula, J. R., De Maziére, A. M., Peden, A. A., Ervin, K. E., Advani, R. J., van Dijk, S. M., Klumperm an, J., &Scheller, R. H. (2004). Rab14 is involved in membrane trafficking between the Golgi complex and endosomes. *MBoC*, *15*(5), 2218–2229.doi.org/10.1091/mbc.e03-10-0777.

30. Grant, B. D., & Donaldson, J. G. (2009). *Pathways and mechanisms of endocytic recycling. Nature Reviews Molecular Cell Biology, 10(9), 597–608.* doi:10.1038/nrm2755.